Semiclassical analysis of spectral correlations in mesoscopic systems

Nathan Argaman,* Yoseph Imry, and Uzy Smilansky
Department of Nuclear Physics, The Weizmann Institute of Science, Rehovot 76100, Israel
(Received 21 February 1992)

We consider the recently developed semiclassical analysis of the quantum-mechanical spectral form factor, which may be expressed in terms of classically definable properties. When applied to electrons whose classical behavior is diffusive, the results of earlier quantum-mechanical perturbative derivations, which were developed under a different set of assumptions, are reproduced. The comparison between the two derivations shows that the result depends not on their specific details, but to a large extent on the principle of quantum coherent superposition, and on the generality of the notion of diffusion. The connection with classical properties facilitates application to many physical situations.

I. INTRODUCTION

One of the important properties of a disordered mesoscopic sample, in which quantum effects are to be studied, is the spectral correlation function. This quantity has been studied by Altshuler and Shklovskii[1] (henceforth AS), for noninteracting electrons, using the perturbative, diagrammatic method. In this work we rederive and extend their results, using the semiclassical method. We consider the problem of an electron in a disordered metal, and extend the results, e.g., to the case of an applied magnetic field. We assume that the elastic mean free path of the electron in the metal, l, is large relative to the Fermi wavelength, $k_F l \gg 1$ (recall that $k_F \propto \hbar^{-1}$).

For orientation purposes, the results for the spectral form factor $\tilde{K}(t)$ (Fourier transform of the correlation function) are sketched in Fig. 1. Three distinct regimes are identified on the time axis: the quantum regime, the ergodic regime, and the diffusive regime. The quantum regime covers times later than the Heisenberg time t_H, which corresponds to the inverse level spacing. The ergodic regime covers times earlier than t_H but later than the ergodic time $t_{\rm erg} = L^2/D$, which is the time required for the diffusive motion to fill all of the available phase space, for a sample of linear dimension L and diffusion constant D ($t_{\rm erg}$ is the inverse of the Thouless energy $\hbar D/L^2$). The diffusive regime extends from $t_{\rm erg}$ down to the mean free time τ. Corresponding regimes can also be identified on the energy axis. As can be seen in the figure, the results for the ergodic and quantum regimes, including the crossover between them, are described well by the theory of random matrices[2] (the applicability of random matrix results to disordered mesoscopic systems has been proved by Efetov,[3] using field-theoretic techniques). In the present work we will be interested in the deviations from the random matrix ensemble results, which occur for times around the ergodic time $t_{\rm erg}$ and earlier (we will also briefly discuss the results for the ergodic regime). As we shall see, the semiclassical method will allow us to derive results for such times for any classically chaotic system, but here we concentrate on the application to diffusive systems. We do not discuss the problem of Anderson localization, i.e., we will always consider samples that are smaller than the localization length, if localization occurs [this is equivalent to requiring $t_{\rm erg} \ll t_H$ (Ref. 4)]. We also neglect interactions such as electron-electron interactions, except for the allowance of a self-consistent potential.

The semiclassical method has been developed by Gutzwiller,[5] Berry,[6] and others for classically chaotic systems. The applicability of random matrix results for such systems in the ergodic regime has been proved,[6] by using a sum rule due to Hannay and Ozorio de Almeida.[7] Recently, Dittrich and Smilansky[8] generalized this result to a special case of a diffusive system (the kicked rotor). Consequently, the semiclassical expressions for a general chaotic system were derived, and applications to specific systems are now being studied (Refs. 9, 10, and the present paper). Note that in this work we use the term "semiclassical approximation" in the strict sense, implying a stationary phase integration around classical paths

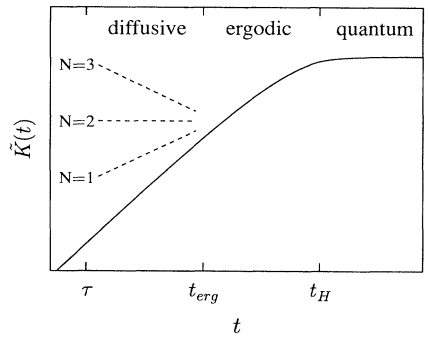

FIG. 1. Sketch of the spectral form factor as a function of time. Full line, orthogonal random matrix ensemble result; dashed lines, modification of random matrix results for classically diffusive systems in N dimensions. The three different time regimes are indicated, and the transition times between them are identified: the Heisenberg time $t_H \sim \hbar/\Delta$ (inverse level spacing) and the ergodic time $t_{\rm erg} \sim L^2/D$ (inverse Thouless energy). The low end of the diffusive regime, the mean free time τ, is also indicated. Both axes are logarithmic, and the case of time-reversal symmetric systems is presented.

that are completely specified by their initial position and momentum. Our approach thus differs not only from the perturbative method but also from the approach of Chakravarty and Schmid,[11] in which only the motion between the scatterers is treated semiclassically, and the impurities are taken as isotropic pointlike scatterers. The work of Chakravarty and Schmid deals with weak localization, and all of these approaches can also be usefully applied to the problem of universal conductance fluctuations,[12] but in the present work we limit the discussion to the spectral form factor. This two-level statistic directly determines many physical thermodynamic and transport properties of the sample (e.g., a contribution to the conductivity and its fluctuations,[1,12] and to the orbital magnetic response[13–16]), in the noninteracting electron picture.

In the following section we present the semiclassical formula for the spectral form factor. We attempt to include enough details (some in the Appendix) to make the presentation coherent and self-contained, as this work is intended mainly for researchers in solid-state physics, who may be unaware of the developments in the field of semiclassical quantization of chaotic systems.[17,18] In the third section we apply the result to a diffusing electron and recover the results of AS, including some effects of, e.g., magnetic fields. The fourth section compares the present work with the perturbative approach of AS, both qualitatively and quantitatively, revealing significant implications for both approaches. In the fifth section we compare our theory with numerical simulations, which are performed for a periodically time-dependent system, and thus refer to the correlations of quasienergy levels. In the last section we conclude and identify some topics for future research.

II. SEMICLASSICAL ANALYSIS OF THE SPECTRAL FORM FACTOR

In classical mechanics, all dynamical systems can be categorized as belonging to the groups of "integrable" or "nonintegrable" systems. The nonintegrable systems can be further characterized as "chaotic," "ergodic," "mixing," and so on. The first distinction, between integrable and nonintegrable systems, is also of central importance when dealing with their quantization. For integrable systems, a full set of good quantum numbers (constants of motion) exists, and the spectrum is given by a smooth function evaluated at integer values of its arguments. This results in a lack of correlations between levels of nearby energies, and the two-level form factor is a constant (the semiclassical treatment of the integrable case is also included in Ref. 6).

For nonintegrable systems analyzing the spectrum itself is a very hard task, but its statistical properties may be usefully studied. This was recognized by Bohigas, Giannonni, and Schmit,[19] who demonstrated the applicability of random matrix ensembles[2] for some properties of such spectra (these ensembles were initially introduced by Wigner and Dyson as models for nonintegrable systems with very many degrees of freedom). More recently it has been shown that some information about spectral correlations in "completely nonintegrable systems" (those with all orbits unstable, see below) can be obtained semiclassically.[6] In the present section we discuss the general form of this semiclassical relationship (Sec. II D). It follows directly from three statements which we first recall (Secs. II A–II C).

A. Representation of the density of states by Gutzwiller's sum

We shall consider the density of states

$$d(\epsilon)=\sum_n \delta(\epsilon-\epsilon_n) \tag{1}$$

and its Fourier transform

$$\tilde{d}(t)=\frac{1}{2\pi\hbar}\int d\epsilon\, d(\epsilon)e^{-i\epsilon t/\hbar}=\frac{1}{2\pi\hbar}\sum_n e^{-i\epsilon_n t/\hbar} . \tag{2}$$

In terms of the propagator $G(x,x',t)=\sum_n \psi_n^*(x)\psi_n(x')e^{-i\epsilon_n t/\hbar}$ (note that we use this definition for both negative and positive times), the latter can be written as

$$\tilde{d}(t)=\frac{1}{2\pi\hbar}\int dx\, G(x,x,t) . \tag{3}$$

Since the propagator can be approximated by a sum over classical paths, this formula enabled Gutzwiller[5] to approximate the density of states in a similar fashion. Note that the semiclassical expression is accurate only if the potential is smooth on the scale of a typical wavelength. As discussed in Sec. IV, this should not be considered a serious limitation (at least within our context).

The averaged density of states (one state per Planck cell) is given by the shortest classical paths (those that take no time to go from x to x). The fluctuations in the spectral density are given by the paths that follow periodic orbits. We shall distinguish between periodic paths, which may be identified by a starting point in phase space and a period T after which the system returns to the same point in phase space, and periodic orbits which are continuous families of such periodic paths (all the periodic paths included in one orbit share a similar geometry). The fluctuating part of the density of states is written as a discrete sum over the periodic orbits, with each term in the sum representing the contribution of all the paths included in that orbit (and their vicinity). Ignoring the averaged density of states, one gets an expression of the form

$$d(\epsilon)=\sum_j A_j(\epsilon)e^{iS_j(\epsilon)/\hbar} , \tag{4}$$

where j is an orbit index, and A_j,S_j are the amplitude and action of that orbit; see below.

In chaotic systems, the paths belonging to an orbit j and to an energy ϵ form a closed curve in phase space. The different paths belonging to the same orbit share the same period, $T_j(\epsilon)$, and differ only in their starting point along the orbit (or conversely by translation in time). This is exactly where our assumption of chaotic behavior enters: we assume that all periodic paths of energy ϵ

form one-dimensional curves (orbits) and are thus unstable. It is well known that if the phase space contains even a single stable path, it will also contain orbits which are sheets of higher dimension.[17,18,20] In the extreme case of integrable systems, all the periodic paths form N-dimensional tori in phase space, where N is the dimensionality or the number of degrees of freedom of the system. For this reason, we assume $N>1$ (all time-independent systems with one degree of freedom are integrable).

By explicitly evaluating (using the stationary phase approximation) the contribution to Feynman's path integral from the vicinity of these unstable orbits, Gutzwiller,[5,18] obtained the following explicit semiclassical expressions for the amplitudes and phases. The phase for an orbit j is $(1/\hbar$ times) the classical action integral

$$S_j(\epsilon)=\oint p\,dq\ , \tag{5}$$

where the integral is taken around the periodic orbit in phase space. In the following, we will use the important property of this classical action, that its derivative gives the period of the orbit[20]

$$\frac{dS_j}{d\epsilon}=T_j(\epsilon)\ . \tag{6}$$

The amplitude is given by

$$A_j(\epsilon)=\frac{T_{j'}(\epsilon)}{2\pi\hbar}|\det[M_j(\epsilon)-I]|^{-1/2}e^{-i\pi\nu_j/2}\ . \tag{7}$$

The derivation of this expression is briefly discussed in the Appendix. The matrix M_j is called the monodromy matrix, and describes the stability of the orbit. For long orbits, the factor $|\det(M_j-I)|$ may be simply approximated by $e^{\lambda T_j}$, with λ a sum of positive Lyapunov exponent(s) characterizing the orbit.[17,18,20] The other factor appearing, $T_{j'}$, originates from the integral over space, and gives simply the length of the classical closed orbit in phase space (measured by the time taken to traverse it). The orbit j may be a repeated orbit, which means that its paths circulate $m_j\neq 1$ times around a primitive orbit which we denote by j' (m_j is called the repetition number). We have $S_j=m_jS_{j'}$, $T_j=m_jT_{j'}$, $M_j=M_{j'}^{m_j}$, and $\nu_j=m_j\nu_{j'}$, and m_j can take any integer value except zero. Note that A_j is not defined here as positive: we include in it a phase factor of $\exp(-i\pi\nu_j/2)$, where ν_j is the (integer) Maslov index.[17,18,21] The amplitude A_j is due to the Gaussian integral around the stationary phase (classical) path.

The domain of validity of the above semiclassical expressions [Eqs. (4)–(7)] is not completely known. In principle, they may fail whenever two (or more) orbits appear too near to each other, and nonquadratic terms in the action become important. It may also fail in applications in which extreme accuracy is needed, and higher-order terms in $\hbar$ are important. Both problems may be expected to become more severe for longer and longer orbits.

At first sight, it seems that the exponential sensitivities characteristic of chaotic behavior lead, already at times of order $\ln(1/\hbar)$ (the Ehrenfest time) to a spreading of any initially minimal wave packet so as to cover the whole available phase space. Conversely, the number of periodic orbits proliferates exponentially, and so if each of them is considered to occupy a phase-space volume proportional to a positive power of $\hbar$, they will have to coalesce at times of the order of $\ln(1/\hbar)$. This argument is, in fact, too crude. When the trace of the propagator is expressed as an integral over phase space, the contributions of different periodic orbits turn out to be additive, so the stationary phase method can be safely applied even when the regions of integration for different orbits overlap. There is also numerical evidence that times of order $\ln(1/\hbar)$ do not signal the breakdown of the semiclassical method, but only of near classical behavior.[22] In fact, the results of the present paper give an additional indication that the semiclassical argumentation remains valid for much longer times.

More serious problems arise concerning much longer orbits, with times longer than the inverse of a typical level spacing $\sim\hbar/\Delta$ ($\Delta=\langle d\rangle^{-1}$, and $\langle d\rangle$ is an averaged density of states). This time is referred to as the Heisenberg time t_H, since it is connected to the mean level spacing by Heisenberg's uncertainty relationship. For such long times, it is clear that the propagator must behave quasiperiodically, with the individual eigenstates and eigenenergies showing up, and it is not clear if (and how) the semiclassical method can reproduce this behavior. This problem will be discussed in future work.[23]

Another problem which must be overcome is that Gutzwiller's sum is absolutely divergent, and in the absence of a well-defined ordering of the periodic orbit terms, cannot be considered to have a well-defined limit at all. In this paper we will generally avoid this problem by introducing Gaussian averaging over small ranges in energy ϵ, which will regain convergence by giving, in every term of the sum, an extra factor which is exponentially small in T_j^2 (a long time cutoff, $\tau_\phi\sim\hbar/\gamma$, was used also in Ref. 1). Eventually we will use convergent expressions containing information about spectral correlations, for which only orbits of lengths smaller than the Heisenberg time contribute.

The resolution of these problems (e.g., by a ressumation of the divergent series) is a central theme in current quantum chaos research.[24] For the purposes of the present work, we shall simply define a time $t_{\rm SC}$, up to which we shall assume that the semiclassical approximation is valid. Beyond that time we assume that the higher-order corrections become of the same order of the results themselves (we discuss here the generic case, and ignore special systems that have an exact semiclassical representation[25]). For the purposes of the present work we will assume that $t_{\rm SC}$ is larger than the ergodic time $t_{\rm erg}$. This is a natural assumption for small $\hbar$, because $t_{\rm SC}$ may be expected to grow as a power of $\hbar^{-1}$,[26] while $t_{\rm erg}$ is $\hbar$ independent (we thus assume that $t_{\rm SC}$ is much larger than the Ehrenfest time, which grows only logarithmically in $\hbar$ and remains much smaller than $t_{\rm erg}$ in most mesoscopic systems). As a result of the comparison with the perturbative method in Sec. IV, we will be able to shed some light on the situation in the context of the present application.

B. Berry's formula for the spectral form factor

Consider the spectral correlation function

$$K(E,\epsilon)=d\left[E+\frac{\epsilon}{2}\right]d\left[E-\frac{\epsilon}{2}\right]. \tag{8}$$

Often this function is averaged over a range in E or over an ensemble to yield a smooth dependence which represents the spectral correlations in a statistical sense (in our notation the averaging will be implicit as explained below). Since this function has two energy variables, one of them may be transformed to yield a quantity with a well-defined energy and time, called the two-level form factor (our definition differs from Ref. 2 by a sign and an additive constant), or simply the spectral form factor:

$$\tilde{K}(E,t)=\frac{1}{2\pi\hbar}\int d\epsilon\, K(E,\epsilon)e^{-i\epsilon t/\hbar}. \tag{9}$$

As $K(E,\epsilon)$ is real and symmetric in ϵ, $\tilde{K}(E,t)$ is also real and symmetric in t, and we shall henceforth restrict attention to positive values of t. Because of the bilinearity of $\tilde{K}$ in $d(\epsilon)$, it contains information about two point correlations of the spectrum, and one may obtain from it two point statistics, such as the spectral rigidity.[6]

By inserting the semiclassical approximation for $d(\epsilon)$ in the above Fourier transform, and noting that all factors are slowly varying except for the phase $S_j\simeq S_j(E)+T_j(E)\epsilon/2$, Berry[6] obtained

$$\tilde{K}(E,t)\simeq\int\frac{d\epsilon}{2\pi\hbar}e^{-i\epsilon t/\hbar}\sum_j A_j e^{i(S_j+T_j\epsilon/2)/\hbar}\sum_k A_k^* e^{-i(S_k-T_k\epsilon/2)/\hbar}=\sum_{jk}A_j A_k^* e^{i(S_j-S_k)/\hbar}\delta[t-\tfrac{1}{2}(T_j+T_k)]. \tag{10}$$

The Taylor expansion of the phase implies a restriction to small values of ϵ (for example, we shall be interested in values of ϵ proportional to positive powers of $\hbar$). Alternatively, we may consider the resulting $\tilde{K}$ as averaged over a small range Δt in the time variable. Although Eq. (10) is sufficient for our purposes, we note that each term here has a rapidly varying phase, and thus all terms with $|T_j-T_k|>\hbar/\Delta E$ may be discarded by averaging over a small range ΔE in energy.[27]

Following Berry, we wish to obtain the "classical" approximation for this expression, by assuming that the contributions to the sum with j different from k have randomly varying phases, and will vanish upon averaging. The assumption here is that there is no correlation between S_j and the other S_k's, and that the averaging is over a wide enough range[28] to render the fluctuating terms negligible. Such correlations will exist when different orbits are related to one another by some symmetry, as discussed below. The ranges of validity of the "classical" approximation of $\tilde{K}(t)$ are similar in many aspects to those mentioned above for the semiclassical expressions for $d(\epsilon)$: for times shorter than the Ehrenfest time, $\hbar$ is small enough so that all the factors $\exp[i(S_j-S_k)/\hbar]$ have random phases and may thus be considered small; for later times, due to the proliferation of the orbits, there are many terms with $S_j-S_k\sim\hbar$, but they may still be ignored if a lack of correlations is assumed (at least in an ensemble-averaged sense); for even longer times, $t\gg t_H$, the behavior changes, and the "classical" approximation fails. Note that, as will become clear below from the comparison with the random matrix results, we have independent evidence that the "classical" approximation is valid throughout the ergodic regime, up to times of the order of t_H. This statement is independent of the inaccuracy of the off-diagonal ($j\neq k$) terms, which becomes large for times later than $t_{\rm SC}$ ($t_{\rm SC}$ may in principle be smaller or larger than t_H).

For systems without any symmetry, omitting $j\neq k$ terms gives just the diagonal part of the sum:

$$\tilde{K}(E,t)\simeq\sum_j |A_j(E)|^2\delta(t-T_j). \tag{11}$$

We shall see later that this expression allows for some coherent quantum interference, and therefore we keep the quotes in calling it "classical." The appearance of $|A_j|^2$ here (and $A_jA_k^*$ above) motivates us to refer to this quantity as a "quantum probability to perform periodic motion."

For time-reversal symmetric systems, the result is modified, since for each orbit j there is another one j^T, which is its time reverse and has an identical amplitude and phase. Thus the off-diagonal terms with $k=j^T$ contribute the same amount as the diagonal terms with $k=j$, and the result is doubled:

$$\tilde{K}^T(E,t)=2\sum_j |A_j(E)|^2\delta(t-T_j) \tag{12}$$

(the superscript T stands for time-reversal symmetry). This is a result of coherent quantum interference between pairs of orbits, and the resulting factor of 2 is very familiar by now.

We mention one additional example of symmetry, which arises for systems with spatial periodicity, in which each orbit j has many replicas with the same geometry and the same amplitudes and phases, which are simply displaced by a lattice vector (an example is discussed in Ref. 8). If the system consists of L periods (and periodic boundary conditions are assumed), then the total result will be L times larger, because for each orbit j there are $L-1$ off-diagonal contributions equal to the diagonal one (another way of stating this is that each family of L replica orbits contributes coherently, $\propto L^2$). This should reconstruct the correlations between levels in such systems, which are known to have highly correlated spectral bands. We shall not discuss such systems further in the present work.

C. Generalization of Hannay and Ozorio de Almeida's sum rule

The "classical" sum appearing above has been calculated by Hannay and Ozorio de Almeida[7] (subsequently referred to as HO), for ergodic systems. The derivation is based on carefully identifying the classical counterparts of the quantity which we have called the "quantum probability to perform periodic motion," and its contribution from each specific closed orbit. Originally, the property of ergodicity (or more exactly, the principle of uniformity that HO present) was used to calculate the "classical" sum. In this subsection we rephrase part of their derivation in a manner that will enable us (in the next subsection) to evaluate the sum for a general chaotic system, in terms of the classical probability to perform periodic motion in that system.

For classical motion, if a system starts at a specific point in phase space r_0, and evolves for a time t, it will reach a new point, denoted by $r_t(r_0)$. It is convenient (especially for ensemble-averaging purposes) to define the distribution function for the system in phase space as $\delta^{2N}(r-r_t)$, and on the energy hypersurface as $\delta^{2N-1}(r-r_t)$. The last δ function is only defined on a certain energy surface, and is undefined if $H(r)\neq H(r_t)$ (we have $\delta^{2N}(r-r_t)=\delta^{2N-1}(r-r_t)\delta[H(r)-H(r_0)]$). Since r is a phase-space coordinate, $r_t=r_0$ implies periodic motion of period t. The averaged classical probability density to perform periodic motion of period t at an energy E is thus given by evaluating the above distribution function at $r=r_0$ and averaging over the energy hypersurface:

$$p(t)=\left[\frac{d\Omega}{dE}\right]^{-1}\int d^{2N}r_0\delta[H(r_0)-E]\delta^{2N-1}(r_0-r_t)\ , \tag{13}$$

where the energy dependence of $p(t)$ is implicit, and $d\Omega/dE=\int d^{2N}r_0\delta[H(r_0)-E]$ is the "area" of the energy hypersurface [the dimensions of $p(t)$ are that of a probability density per unit hypersurface area]. It is clear that the integral in Eq. (13) has a contribution from every point which lies on a periodic orbit of period t, and we define the contribution of the entire periodic orbit j by

$$P_j(E,t)=\int_{\Gamma_j} d^{2N}r_0\delta[H(r_0)-E]\delta^{2N-1}(r_0-r_t)\ , \tag{14}$$

where Γ_j is the region in phase space near the orbit j (this integral is dimensionless, and will vanish if $T_j\neq t$). We call this the classical probability to perform periodic motion along the orbit j (these probabilities are simply related to HO's intensities).

A direct evaluation of this quantity may be performed (see, e.g., Ref. 17), and is included in the Appendix for completeness. It gives

$$P_j(E,t)=\delta(t-T_j)T_{j'}|\det(M_j-I)|^{-1}\ , \tag{15}$$

where again T_j is the period of the orbit, M_j is its monodromy matrix, and j' refers to the primitive orbit corresponding to j. The factors appearing here are easily understandable—the $T_{j'}$ represents the "number" of different paths that start at different points around the periodic orbit, and the monodromy matrix represents its stability. The appearance of the same matrix determinant (and the same period) as in the result for Gutzwiller's amplitude [Eq. (7)] will play a crucial role in the following.

D. The relationship between the spectral form factor and the classical probability for periodic motion

The expressions for the quantum and classical contributions of an orbit j to the probability to perform periodic motion are very similar. This enables us to reach the main result of this section at once: Combining Berry's formula, Eq. (11), with Gutzwiller's result for the probability amplitudes, Eq. (7), gives

$$\begin{aligned}\tilde{K}(E,t)&\simeq\sum_j|A_j(E)|^2\delta(t-T_j)\\&=\sum_j\frac{T_{j'}^2}{(2\pi\hbar)^2}|\det(M_j-I)|^{-1}\delta(t-T_j)\ ,\end{aligned} \tag{16}$$

and comparing this with HO's classical probability for each orbit, Eq. (15), gives

$$\tilde{K}(E,t)\simeq\sum_j\frac{T_{j'}}{(2\pi\hbar)^2}P_j(E,t)\simeq\frac{|t|}{(2\pi\hbar)^2}\frac{d\Omega}{dE}p(t)\ . \tag{17}$$

In the last step we have neglected the contribution of orbits with high repetition numbers ($|T_j|\neq T_{j'}$), which is justified due to the exponential proliferation of primitive orbits.[7] The factor of t between the quantum and classical result has its origin in the constructive interference of the "t periodic paths" that belong to the same "family," denoted here by the periodic orbit j (recall that the factors of $2\pi\hbar$ originate in the definition of the Fourier transform, and the $d\Omega/dE$ factor is due to the definition of the averaging over an energy surface). These paths all have the same amplitude and phase, and therefore the quantum result is proportional to t^2 and the classical one only to t. Note that each orbit contains in fact a continuous infinity of different paths, and therefore one must go into the detailed calculation above to show that indeed they may be considered as "t different paths" with the same amplitude and phase.

As already mentioned, in systems with time-reversal symmetry, the result is modified, since the orbits are arranged in pairs related by time-reversal symmetry. Constructive interference occurs not only between the paths within each orbit, but also between paths belonging to the two different orbits in the same pair. As a result, the ratio of the quantum to the classical result is increased by a factor of 2:

$$\tilde{K}^{T}(E,t)\simeq\frac{2|t|}{(2\pi\hbar)^2}\frac{d\Omega}{dE}p(t)\ , \tag{18}$$

where, again, the T superscript signifies time-reversal symmetry.

The identification of the classical probability [$p(t)$] and quantum interference (t) factors in the above semiclassical formulas [Eqs. (17) and (18)] facilitates application to a wide range of systems. An application to a one-

dimensional, periodically time-dependent, diffusive system is given by Dittrich and Smilansky.[8] Current work includes an application to composite systems, in which the phase space contains a few weakly interacting chaotic regions,[9] and to diffusion in a quasi-one-dimensional system.[10] Before the application to mesoscopic systems is presented in the next section, we wish to recall some aspects of the original discussion of ergodic systems.

In the strict semiclassical limit, $\hbar \to 0$, the separation between nearby energy levels becomes very small ($\sim \hbar^N$), and the relevant times in $\tilde{K}(t)$ become very large ($\sim \hbar^{1-N}$). Thus all classically definable times, those which do not involve $\hbar$ in any way ($\sim \hbar^0$), become "semiclassically small" in comparison. For chaotic systems, the largest classically definable time is $t_{\rm erg}$, the time for the particle to reach all points in its available phase space (in the original works[6,7] this and all earlier times were considered as "short," and the behavior in this regime was considered "nongeneric," as it depends on the classical details, such as the diffusive property). For times longer than $t_{\rm erg}$ the behavior is ergodic, and the distribution function is uniform over the energy surface $\delta^{2N-1}(r_t - r) \simeq 1/(d\Omega/dE)$. This gives $p(t) = (d\Omega/dE)^{-1}$ and accordingly $\tilde{K}(E,t) \simeq t/(2\pi\hbar)^2$, which results in $K(\epsilon) \propto \epsilon^{-2}$, and a logarithmic spectral rigidity (see Ref. 6). This defines the behavior of the spectral correlations in the classically ergodic regime, and agrees, as already mentioned, with the results of random matrix theories (see Fig. 1).

It is illuminating to point out how the different classical paths contribute to these results.[29] As we mentioned, the determinants involved in the denominator of P_j represent the instability of the motion and increase exponentially with time, at a rate given by the positive Lyapunov exponent(s). On the other hand, the "number" of periodic paths of period within Δt of t increases exponentially as $\Delta t \exp(\alpha t)$, where α is called the topological entropy of the system. The cancellation of these two exponentials to give a constant $p(t) = (d\Omega/dE)^{-1}$ is a ramification of a result well known from classical mechanics of closed ergodic systems, namely that the (sum of) Lyapunov exponent(s) is equal to the topological entropy.[20] As mentioned above, the quantum-mechanical probability to follow periodic motion is now obtained by grouping these paths into $(\Delta t/t)\exp(\alpha t)$ orbits of size t. The constructive interference within each orbit gives a factor of t^2, which is combined with the $1/t$ from the subdivision into orbits, to give the result of $\tilde{K}(t) \propto t$.

The results given above for the spectral form factor increase linearly with t, apparently without limit. For late times, it is clear that this result is not valid, and $\tilde{K}(t)$ must approach a constant. Berry[6] gives a detailed mathematical proof of this statement, and calls it a "semiclassical sum rule." Here we will just note that for a finite system, when t is much larger than the Heisenberg time $t_H = 2\pi\hbar\langle d \rangle$, the form factor no longer represents the correlations between the levels, but rather the "shape" of each one of them. For sharp (δ function) levels, the form factor in this quantum regime will simply be a constant ($\langle d \rangle/2\pi\hbar$). This can be understood in analogy to the form factor of a one-dimensional gas, in which every atom in space represents a level in energy (for large momenta it approaches the atomic form factor). Such an analogy was found useful in treating random matrix ensembles.[2]

As shown by Berry,[6] the combination of the linear increase and the eventual saturation to a constant reproduces the results of the appropriate random matrix ensembles (if the form of the interpolation between these two extremes is chosen correctly).

The result of Eqs. (17) or (18) is very powerful, even when the limitation to early times is acknowledged, and can provide predictions on spectral correlations for many systems whose classical behavior is known. In the next section we illustrate this by discussing the case of a particle whose motion is diffusive in the classical limit.

III. APPLICATION TO A DIFFUSING ELECTRON

In this paper we are interested in applying the above semiclassical results to electrons in disordered solids. We will use the notion of diffusion to describe all necessary classical properties of the motion. The assumption of diffusive behavior in a disordered mesoscopic sample appears to be an excellent assumption for a large variety of random potentials and scatterers (for times longer than the transport mean free time). In this section we discuss regular and anomalous diffusion, as well as some effects of external fields. For simplicity, we ignore the spin degeneracy of the electrons (it can be accounted for simply by multiplying by a factor of 2 for the spectral density, and a factor of 4 for the spectral form factor).

For a diffusing particle in N dimensions (having N degrees of freedom), the probability distribution over the phase-space energy surface is a spreading Gaussian in real space and uniform in momenta. For long times the electron will diffuse over the whole sample, the system becomes ergodic, and the results discussed in the preceding section are applicable. But for a diffusive mesoscopic sample with a small but finite $\hbar$ (and hence a finite wavelength $\lambda_F = \hbar/p_F$) and a large but finite size L, we are also interested in times shorter than the time for diffusion across the sample $t_{\rm erg} = L^2/D$. For such times the distribution is

$$\delta^{2N-1}(r - r_t) \simeq \left[\frac{d\Omega_p}{dE}\right]^{-1} \frac{1}{(4\pi D t)^{N/2}} \times \exp\left[\frac{-(x - x_0)^2}{4Dt}\right], \tag{19}$$

and since this is independent of the specific starting point $r_0 = (x_0, p_0)$ (at least far from the boundaries), we get the result for $p(t)$ by simply setting $r = r_0$. Note that the distribution over the "angular variables" of the momenta is given by a constant, the inverse of the free-particle density of states $(d\Omega_p/dE)^{-1}$, and will cancel out in the following ($\Omega = \Omega_x \Omega_p$ is the decomposition of phase-space volume into coordinate and momenta spaces). Finally, we find for the diffusive regime

$$\tilde{K}^{T}(E,t)\simeq\frac{2t}{(2\pi\hbar)^2}\frac{\Omega_x}{(4\pi Dt)^{N/2}}$$

$$=\frac{2\Omega_x}{(2\pi\hbar)^2(4\pi D)^{N/2}}t^{1-N/2}\ . \tag{20}$$

We have assumed that the system obeys time-reversal symmetry, as will happen for an electron in a nonmagnetic metal at zero magnetic field. This result is identical to that obtained by Altshuler and Shklovskii[1] using the less transparent diagrammatic method (see Sec. IV). As a function of ϵ we have $K(E,\epsilon)\simeq-(\pi\epsilon)^{-2}$ for $\Delta\lesssim\epsilon\lesssim E_C$ (ergodic regime), and $K(E,\epsilon)\simeq C_N\epsilon^{N/2-2}$ for $E_C\lesssim\epsilon\lesssim\hbar/\tau$ (diffusive regime), where $E_C=\hbar/t_{\rm erg}$ is the Thouless energy and C_N is a constant that depends on the number of dimensions.

Notice that the result is always enhanced relative to the ergodic case, since the distribution tends to stay concentrated around the starting point, until such late times as to make it evenly distributed over the whole volume. This immediately gives us the time of transition—that which gives $(4\pi Dt)^{1/2}$ equal to the size of the system L (cf. Sec. III B below). To find the exact form of this crossover, all we must do is calculate the appropriate $p(t)$ by averaging the classical probability to return over the volume, taking account of the boundary conditions.

The simple expression for the spectral form factor, Eq. (20), is the principal result of this section, which we wish to present and discuss. In this section we discuss theoretical predictions for various modifications of the above, such as by a static magnetic field, or a fractal-like geometry. In the next sections we compare Eq. (20) with the earlier theoretical derivation and with numerical results.

A. Persistent currents

An interesting application involves a magnetic field in an Aharonov-Bohm ring geometry. The persistent current flowing around such a ring in thermodynamic equilibrium is now within reach of experiments,[30,31] and was recently calculated, using the diagrammatic perturbative method. We give here an alternative derivation for two calculations, one for the typical current in the context of the grand-canonical ensemble,[15] and the other for the averaged current in the context of the canonical ensemble[16] (the remarkable paramagnetic response obtained in the canonical ensemble is intimately connected with the magnetic-field sensitivity of the spectral correlations discussed in this subsection and in the next one, and is the subject of recent increased interest[32]).

The persistent current in the grand-canonical ensemble is given by $I=-c\partial\Omega/\partial\phi$, where ϕ is the Aharonov-Bohm flux in the ring and Ω is the free energy. At zero temperature, the free energy is given by $\Omega=\int_{-\infty}^{0}d\epsilon\,\epsilon d_\phi(\epsilon)$ (ϵ is measured from the Fermi energy). The flux-dependent density of states is given, within the semiclassical approach, by the sum over periodic orbits with an extra flux-dependent phase, $d_\phi(\epsilon)\simeq\sum_j A_j\exp(iS_j/\hbar+i2\pi n_j\phi/\phi_0)$, where n_j is the winding number of the orbit j, and $\phi_0=hc/e$ is the flux quantum. The average of this current I over the impurity positions was found to be exponentially small,[15] as is indeed plausible because of the random phases involved in the sum over orbits.[33] We now calculate the typical current, by performing the impurity average over the square of this current:

$$\langle I^2\rangle\simeq c^2\frac{\partial}{\partial\phi}\frac{\partial}{\partial\phi'}\int_{-\infty}^{0}d\epsilon\,\epsilon\int_{-\infty}^{0}d\epsilon'\epsilon'\left\langle\sum_{j,k}A_jA_k^{*}e^{i(S_j-S_k)}e^{i2\pi(n_j\phi-n_k\phi')/\phi_0}\right\rangle, \tag{21}$$

where the orbit j is taken at energy ϵ and the orbit k at energy ϵ' (the fluxes of the two orbits, ϕ and ϕ', are both set equal to the Aharonov-Bohm flux after the derivatives are taken). Our reasoning now implies that all terms with k different from both j and its time reverse j^T have wildly fluctuating phases due to the different actions, and do not contribute. We use the diffusive approximation for the motion of the electrons along the length of the wire (the circumference of the ring), assuming that the diffusive motion fills the much smaller transverse dimensions of the wire within a time much shorter than $t_{\rm erg}$. The orbits are grouped according to their winding number, and we find (using $n_{j^T}=-n_j$, and omitting the j subscript)

$$\langle I^2\rangle\simeq c^2\int_{-\infty}^{0}d\epsilon\,\epsilon\int_{-\infty}^{0}d\epsilon'\epsilon'\int_{-\infty}^{\infty}dt\,e^{it(\epsilon-\epsilon')/\hbar}\sum_{n=-\infty}^{\infty}\frac{|t|}{(2\pi\hbar)^2}\frac{L}{\sqrt{4\pi D|t|}}\exp\left[-\frac{n^2L^2}{4D|t|}\right]\left[\frac{2\pi n}{\phi_0}\right]^2(1-e^{i4\pi n\phi/\phi_0}) \tag{22}$$

(L is the circumference of the ring). As usual, we have introduced the Fourier transform of the spectral correlation function, and we use the value of the diffusion constant D applicable to electrons at the Fermi surface, because electrons at lower energies do not contribute significantly. The integrals are now simply evaluated, and for zero temperature [$\int_{-\infty}^{0}\epsilon\,d\epsilon\,e^{it\epsilon/\hbar}\simeq(\hbar/t)^2$] the result is

$$\langle I^2\rangle\simeq\sum_{n=1}^{\infty}\frac{24}{\pi^2n^3}\left[\frac{eD}{L^2}\sin(2\pi n\phi/\phi_0)\right]^2. \tag{23}$$

If a finite temperature or a dephasing time is introduced the time integration is exponentially damped at values of t greater than $\hbar/k_BT$ or τ_ϕ, leading to a damping of the high harmonics in this sum (recall that in any case the time integral must be limited by the Heisenberg time t_H, because for longer times the "classical" approximation is inapplicable).

As a result of the measurement of a nonzero ensemble-averaged persistent current in the experiment,[30] modifications of the above arguments were studied. In one case, it was argued that the main effect of the electro-

static interaction between electrons and ions would be to fix the number of electrons on each mesoscopic ring. This number will also be fixed if the rings are decoupled from the substrate. Thus, the canonical ensemble persistent current was studied,[16] and it was shown to be given by $I_{ce}=(-c\Delta/2)(\partial/\partial\phi)(\delta N)^2$. Here $(\delta N)^2$ is the variance of the number of particles, evaluated in the grand-canonical ensemble, which may be written at very low temperatures as $\int_{-\infty}^{0}d\epsilon\int_{-\infty}^{0}d\epsilon' K(\frac{1}{2}(\epsilon+\epsilon'),\epsilon-\epsilon')$. Only the flux-dependent part of $\tilde{K}(E,t)$, which we denote by $\tilde{K}^{\phi}(E,t)$, is important (there is no need to distinguish ϕ from ϕ' in the intermediate stages), and therefore only terms in which pairs of time-reversed orbits appear ($k=j^T$) are retained. Using the same argumentation as above, we find

$$\tilde{K}^{\phi}(E,t)=\frac{t}{(2\pi\hbar)^2}\sum_n\frac{L}{\sqrt{4\pi Dt}}\exp\left[-\frac{n^2L^2}{4Dt}\right]\times\cos(4\pi n\phi/\phi_0)\ . \tag{24}$$

This leads to

$$\langle I_{ce}\rangle\simeq-\frac{c\Delta}{2}\frac{\partial}{\partial\phi}\int_{-\infty}^{0}d\epsilon_1\int_{-\infty}^{0}d\epsilon_2\int dt\, e^{i(\epsilon_1-\epsilon_2)t/\hbar}\tilde{K}^{\phi}(t)=\sum_{n\neq0}I_n\sin(4\pi n\phi/\phi_0) \tag{25}$$

with I_n given by

$$I_n\simeq\frac{c\Delta}{2}\frac{4\pi n}{\phi_0}\int_{-\infty}^{\infty}dt\left|\frac{\hbar}{t}\right|^2\frac{|t|}{(2\pi\hbar)^2}\frac{L}{\sqrt{4\pi D|t|}}\times\exp\left[\frac{-n^2L^2}{4D|t|}\right]=\frac{c\Delta}{\pi\phi_0}\mathrm{sgn}(n)\ . \tag{26}$$

Again, we have considered zero temperature, and ignored the problem of long times, which can be handled either by introducing a dephasing time[16] or by acknowledging that for times $t>t_H$ the spectral form factor $\tilde{K}(t)$ approaches a constant which is independent of ϕ (in this case the results of sophisticated field-theoretic approaches[34] should be mimicked). We note that this result, valid for noninteracting electrons, is a few orders of magnitude short of explaining the experiment.[30,31]

B. Orthogonal-unitary crossover

To further illustrate the power of this approach, we employ it here for an intuitive picture of the breaking of time-reversal symmetry in a disordered mesoscopic sample. It is by now well known from the theory of weak-localization corrections to the conductivity (see, e.g., Ref. 11), that a magnetic field H breaks the symmetry between the time-reversed paths and destroys their interference by introducing extra phase factors. In the context of the random matrix ensembles, this corresponds to a crossover from orthogonal to unitary symmetry. For any periodic orbit j, the diagonal term in the semiclassical sum will not be modified by a constant external magnetic field, while the cross term with the time-reversed partner j^T has an additional factor of $\exp(i4\pi a_jH/\phi_0)$, where a_j is the net area perpendicular to the magnetic field enclosed by the orbit j ($\phi_j=Ha_j$ is the flux enclosed by the orbit). For a given magnetic field H and a given time t (assumed much smaller than the Heisenberg time), we must find the average value of this factor. This averaged phase factor will be real, positive, and smaller than unity (Chakravarty and Schmid define a "quasiprobability" that includes it[11]). For short times, the typical area a_j will be much smaller than the area associated with the magnetic field $L_H^2=\phi_0/H$ (L_H is called the magnetic length), and the additional factor will be approximately unity, so that the results of the time-reversal symmetric case are obtained. In the opposite case of long times the results will be as for nonsymmetric systems. We are interested here in times near the crossover time t_x, between these two extremes. We now discuss two field regimes, in which t_x occurs in the ergodic and the diffusive regimes, respectively.

For weak fields, $L_H\gg L$, and the field produces less than a flux quantum in the area of the system. In order to accumulate a phase of order unity from the magnetic field, the particle has to encircle the sample a net number of times of order L_H^2/L^2. This will happen at times much longer than t_{erg}, for which the classical behavior is ergodic, and the system can be considered as a quantum dot. This is exactly the case of the crossover between the Gaussian unitary ensemble (GUE) and the Gaussian orthogonal ensemble (GOE), which has recently been studied,[35] and in the following we find results which are consistent with this reference for $t_x\ll t_H$.

For ergodic motion we may assume that each orbit returns very near to its starting point many times, each time accumulating a random contribution to its area. The distribution of areas a_j will, according to the central limit theorem, be Gaussian, with the standard deviation proportional to $L^2(t/t_{\mathrm{erg}})^{1/2}$. Calculating the average of the extra factor $\exp(i4\pi a_jH/\phi_0)$ amounts to evaluating the Fourier transform of this distribution, which in this case is simply a decreasing exponential. We thus find that

$$\tilde{K}^{X}(t)=\tfrac{1}{2}[1+\exp(-t/t_x^{<})]\tilde{K}^{T}(t)\ , \tag{27}$$

where the superscript in $\tilde{K}^{X}$ signifies the crossover behavior, and $\tilde{K}^{T}$ is the result for the time-symmetric ($H=0$) case. The crossover time is proportional to

$$t_x^{<}\sim t_{\mathrm{erg}}\left[\frac{L_H}{L}\right]^4\gg t_{\mathrm{erg}}\ , \tag{28}$$

and its exact value depends on the boundary conditions, i.e., on the shape of the sample (a specific example will be given towards the end of this subsection). For fields so small that $L_H/L\gg(t_H/t_{\mathrm{erg}})^{1/4}$, the field will play a role only for very late times $t_x>t_H$, or for correlations between levels separated by much less than the mean separation Δ (Ref. 35) (this holds although the semiclassical argumentation is not valid in this regime).

For strong fields, $L_H\ll L$, the field produces more than a flux quantum in the system (but we consider fields not too strong, so we are still in the diffusive regime,

$L_H \gg l$, where l is the mean free path). In this case the crossover occurs for times in which the motion is diffusive (rather than ergodic), and we shall obtain a different kind of crossover behavior that generalizes Eq. (27) in the same sense that Eq. (20) generalizes the standard GOE results.

In the present case the central limit theorem is not applicable, as we shall see, and we use differential (kinetic-type) equations in order to find the distribution of areas a_j. First, we generalize the notion of area to include open paths (those which start and end at different points) by defining $a_j = \int_j x\, dy$, with the integral taken along the path (taking the z direction along the magnetic field; this corresponds to a choice of gauge in which the vector potential is proportional to $x\hat{y}$). For simplicity we treat the two-dimensional case of motion on a surface $z=$const. In analogy with the derivation of the diffusion equation, we define a distribution for the paths starting from (x_0,y_0) at time $t=0$ and ending at (x,y) at time t, with an area a, and find that this distribution obeys the following differential equation:

$$\left\{\frac{\partial}{\partial t}-D\left[\frac{\partial^2}{\partial x^2}+\left[\frac{\partial}{\partial y}+x\frac{\partial}{\partial a}\right]^2\right]\right\}f(x,y,a,t) = \delta(x-x_0)\delta(y-y_0)\delta(a)\delta(t)\ . \tag{29}$$

This equation turns out to be separable (for the homogeneous case), and can therefore be easily solved (in analogy with the treatment in Ref. 11). The solution is a sum of eigenmodes:

$$f(x,y,a,t)=\sum_{n=0}^{\infty}\int\frac{dk_y}{2\pi}\int\frac{dk_a}{2\pi}e^{ik_a a+ik_y(y-y_0)}\psi_n^*\left[x_0+\frac{k_y}{k_a}\right]\psi_n\left[x+\frac{k_y}{k_a}\right]e^{-\Gamma(n,k_y,k_a)t}\ , \tag{30}$$

with the decay rate of each mode given by

$$\Gamma(n,k_y,k_a)=(2n+1)D|k_a|\ , \tag{31}$$

and ψ_n equal to the normalized eigenfunctions of a quantum harmonic oscillator. Specializing to closed orbits $(x,y)=(x_0,y_0)$ we find for the conditional distribution of the area

$$\begin{aligned} p\{a|(x,y)=(x_0,y_0),t\} &= \frac{f(x_0,y_0,a,t)}{\int da\, f(x_0,y_0,a,t)} \\ &= \frac{\sum_n \int (|k_a|dk_a/4\pi^2)\exp[ik_a a-(2n+1)D|k_a|t]}{(4\pi Dt)^{-1}} \\ &= \frac{d}{da}\frac{1}{[1+\exp(-\pi a/Dt)]}=\frac{\pi/2Dt}{1+\cosh(\pi a/Dt)}\ , \end{aligned} \tag{32}$$

where we have used $\sum_{n=0}^{\infty}1/[x+i\pi(2n+1)]+\text{c.c.}=1/[1+\exp(-x)]-\frac{1}{2}$.

In order to find the behavior of the spectral form factor, we must now average the factor $\exp(i4\pi aH/\phi_0)$ over the above distribution, or in other words restrict our attention to the $k_a=-4\pi H/\phi_0$ component. We find in this case a different form of crossover:

$$\tilde{K}^X(t)=\frac{1}{2}\left[1+\frac{t/t_x^>}{\sinh(t/t_x^>)}\right]\tilde{K}^T(t)\ . \tag{33}$$

The crossover time for strong fields, $t_x^>$, is found to be

$$t_x^>=\frac{\phi_0}{4\pi HD}\sim\frac{L_H^2}{D}\ll\frac{L^2}{D}=t_{\text{erg}}\ . \tag{34}$$

This result is valid for two dimensions with the magnetic field perpendicular to the sample, and also for three dimensions (the same derivation follows through with an extra z dependence where needed). A schematic representation of the crossover in the time versus magnetic-field and the energy versus magnetic-field planes is given in Fig. 2.

In deriving the result [Eq. (33)] we have taken the infinite volume approach, and ignored the boundary conditions, as appropriate for strong fields. In principle it is possible to restore the zero current boundary conditions on the spatial boundary, to choose a specific value of $k_a \propto H$ (as in Ref. 11), and to solve Eq. (29) without taking the strong field approximation. For long times all but the mode with minimal Γ will decay, and for a zero field, $k_a=0$, this mode will be simply a constant (as a function of space) and will not decay, $\Gamma_0=0$. For weak fields we may assume by symmetry $\Gamma_0(k_a)\propto k_a^2$, which implies a Gaussian distribution for the areas. We thus regain the simple crossover result for weak fields [Eq. (27)] without invoking the central limit theorem. For specific geometries we may also calculate the proportionality constant in Eq. (28), by evaluating $\Gamma(k_a)$ for small k_a in perturbation theory. This turns out to be simple for geometries in which it is possible to find a gauge in which the component of the vector potential perpendicular to the boundaries vanishes (this component appears in the boundary conditions[36]). A simple example is that of a circular disk, which gives $t_x^<=L_H^4/2\pi^2DR^2$, where R is the radius of the disk (this is the example used to give the numerical coefficient for Fig. 2).

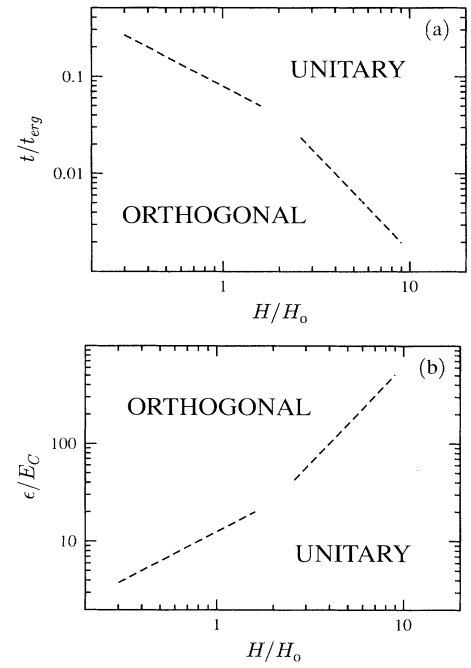

FIG. 2. The regions of approximate orthogonal and unitary symmetry and the crossover regions separating them, in the time–magnetic-field plane for the spectral form factor (a), and in the energy–magnetic-field plane for the spectral correlation function (b). The dashed lines denote $t_x^<$ and $t_x^>$, and the magnetic field, time, and energy have been normalized by $H_0 = A/\phi_0$, $t_{erg} = A/D$, and $E_C = \hbar D/A$ (A is the area of the sample, which is taken as a disk; see the text).

In this subsection, we have developed the results for only one type of crossover, the breaking of time-reversal symmetry (a generalization of the GOE to GUE crossover). This was done in analogy to the averaging over the same field-induced phase factors in the context of weak localization by Chakravarty and Schmid.[11] A very similar derivation would apply to other crossovers, involving symplectic symmetry (GSE). In fact, the results of Chakravarty and Schmid include these cases too[37] (symmetry breaking by spin-orbit and spin-flip scattering).

The different forms of crossover were considered within the diagrammatic approach already by Altshuler and Shklovskii.[1] Their results were derived by developing differential equations for the components of their diagrams ("diffuson" and "cooperon"), and our equation [Eq. (29)] and results are analogous (instead of crossover times for a given magnetic field they estimated crossover magnetic fields for a given energy; they did not consider the detailed forms of the crossovers). The present derivation may help to clarify the physics, by supplying an additional intuitive viewpoint.

C. Anomalous diffusion

The result for the form factor has an interesting dependence on the time [Eq. (20)], which changes from a positive power for low dimensionality to a negative power for $N > 2$. It is also possible to have a fractional dimension in classical diffusion, as happens for electrons diffusing in a fractal geometry,[38] such as in a metal-insulator alloy near the percolation threshold. In the general case, the distribution function spreads to a distance r in a time $t \propto r^{d_{rw}}$, where d_{rw} is called the effective dimensionality of the random walk (the Fickian value is $d_{rw}=2$). Assuming that the distribution fills the volume $s = r^{d_f}$ more or less uniformly, with d_f the fractal dimensionality, the expression for $p(t)$ becomes

$$p(t) \propto t^{-d_f/d_{rw}} . \tag{35}$$

For quantum-mechanical propagation in this geometry, we will have

$$\tilde{K}(t) \propto t^{1-d_f/d_{rw}} . \tag{36}$$

At later times, when the radius of the region covered by the spreading distribution function becomes larger than the correlation length ξ, the results reduce to the previous case $\tilde{K}(t) \propto t^{1-N/2}$.

Another case of classical, anomalous diffusion is, e.g., when local fields are present, which make the diffusion asymmetric.[39] In this case there are potential barriers of height $\sim\sqrt{R}$ at a distance $\sim R$ away from any initial point, and diffusion across such barriers takes an exponentially long time (it is estimated by the use of Arrhenius factors as in thermal activation). This leads to an $\langle R^2 \rangle \propto \ln^4(t)$ behavior, which can again be inserted into the expressions above, yielding the appropriate $\tilde{K}$.

Note that anomalous diffusion arises in different cases as a classical or a quantum-mechanical effect. Since our analysis was semiclassical and relates to classical paths, we claim applicability only to the former type of cases. It would be interesting if a generalization to the quantum anomalous diffusion, e.g., near the metal-insulator transition, would be possible. As the assumptions leading to Eq. (20) were not checked under the circumstances of anomalous diffusion, it would be of interest to check numerically whether our predictions are indeed confirmed. Related work on the Domino Billiard is in progress.[10]

IV. COMPARISON WITH THE PERTURBATIVE APPROACH

Altshuler and Shklovskii (AS, Ref. 1) have calculated the spectral correlation function $K(E,\epsilon)$ for an electron in a mesoscopic sample, using standard methods of perturbative quantum mechanics.[40] They consider an electron propagating in a metal and undergoing scattering by a random impurity potential, utilizing a Feynman diagram technique to enumerate the different terms in perturbation theory. By evaluating a certain set of diagrams (so called "two-ladder" diagrams, with the "ladders" corresponding to "diffusons" or "cooperons"), they found

$$K^T(E,\epsilon) = -\frac{s^2}{\pi^2} \Re \sum_q (\epsilon + i\hbar D q^2 + i\gamma)^{-2} , \tag{37}$$

where the factor $s=2$ is included to account for the spin degeneracy of each level, and γ is a small energy cutoff (physically due to dephasing). This is exactly the Fourier transform of $|t|p(t)$ [Eq. (18)], for the diffusive case [the derivative with respect to ϵ of the (ϵ,q) representation of the diffusion Gaussian $2\Re i/(\epsilon + i\hbar D q^2)$, evaluated at

$x=0$; twice the real part appears because of the symmetry with respect to $t \rightarrow -t$]. By using a sum over discrete momenta applicable to a rectangular sample, rather than an integral over q, AS were able to treat both the diffusive ($t \ll t_{\text{erg}}$; sum $\simeq$ integral) and the ergodic ($t \gg t_{\text{erg}}$; sum $\simeq$ first term) regimes.

In this section we compare some of the details of this derivation with the present semiclassical treatment, and show that they are indeed analogous. We are thinking here of the standard disorder ensemble which is implied by the diagrammatic technique: the potential consists of a large number of similar terms, each corresponding to an impurity centered at a point R_i, with the positions R_i averaged over the volume. We assume that the impurities are small, i.e., most of the propagation is simply free motion between the impurities (but we do not necessarily imply that the impurities are pointlike, which is equivalent to assuming a Gaussian white-noise potential, and significantly simplifies some higher-order diagrams). The analogy is apparent once it is appreciated that, in both the semiclassical and the perturbative approaches, the spectral density of states may be written as a sum and integral over contributions of different paths, where each path is identified by a starting position and a list of impurities on which the path scatters before returning to the starting point. Thus, the diagrammatic calculation is in a sense also a calculation of the "quantum probability to return to the starting point," albeit in a different approximation scheme.

The equivalence of the two approaches becomes exact when both are applied to the diffusive regime. In both cases, the details of the approximate evaluation of the quantum propagation are swept aside: in the semiclassical approach a diffusion Gaussian is used for the classical probability for periodic motion; in the perturbative approach, diffusion-type equations are used to describe the "diffuson" and "cooperon" subdiagrams. The (leading-order) results of the two approaches become identical (as exemplified in Sec. III B). In the following subsections we compare the two approaches in more detail, as we find that this is helpful in developing physical intuition regarding both methods of derivation.

A. Understanding the diagrams

The comparison of the diagrams with the semiclassical method clarifies their physical meaning. The "two-diffuson" and two-cooperon" diagrams considered by AS are reproduced in Fig. 3, together with their representation in coordinate space. We have chosen a specific representative of these diagrams, with seven scattering events, considered to occur at specified points (we postpone the averaging over the coordinates of these impurities to a later stage). To obtain $K(\epsilon)$ one has to trace over the external coordinates x and y (similar integrals have been performed in Ref. 11). It turns out that this integral is contributed mainly from points very close to the straight line connecting the first and last scattering points (e.g., x near the line connecting 1 and 7 in the figure). The result of the integral, to leading order in $1/(k_F l)$, is proportional to a single Green function con-

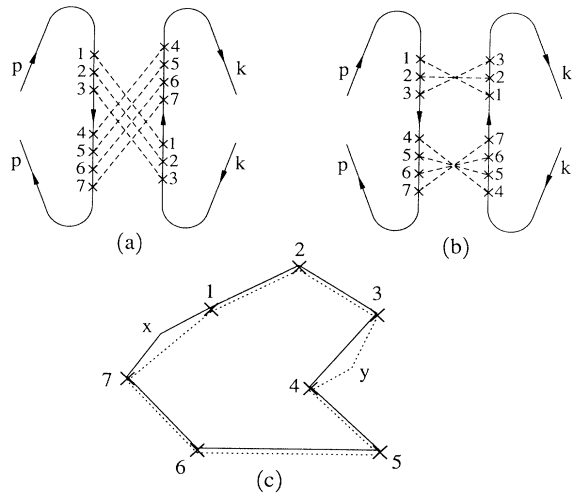

FIG. 3. Comparison of Altshuler and Shklovskii's two-diffuson (a) and two-cooperon (b) diagrams with their spatial representation (c). A representative of the diagrams with seven scattering points has been chosen. The trace over the momenta p and k transforms into an integration of the coordinates x and y over space. After the integration the "triangles" near these points [the triangles $(1,x,7)$ and $(3,y,4)$ in the figure] collapse to form straight lines, i.e., a closed orbit is obtained (see text).

necting these two scattering points, with the constant of proportionality measuring the length of that segment of the closed orbit (in terms of the wavelength). We thus find that, qualitatively, these diagrams describe two closed electron paths that follow the same closed orbit, although they start at different points. Both diagrams correspond to the same periodic orbit, and only the direction of propagation (the arrows) is not identical with the calculation of Sec. II because there we took the complex conjugate of one of the density-of-states factors. The diagrams of Fig. 3, unlike the semiclassical calculation, do not contain the contribution in which the starting point of both paths occurs between the same pair of scattering events (this contribution, which corresponds to diagrams with a single ladder, is small in the diffusive regime).

The analogy with the semiclassical derivation thus yields a physically intuitive way to identify the diagrams which give the leading contribution to the spectral form factor. The analogy naturally generalizes to the extra "two-cooperon diagram" that is included for time-reversal symmetric cases—the two-electron paths correspond there to scattering off the same list of scatterers in opposite order. The development of physical intuition as to the meaning of the diagrams in terms of paths which the electrons can follow is an idea which has been pursued for some time, especially in the context of weak localization.[11,41,42] Here we have reversed the usual approach, and presented the semiclassical derivation as the starting point. Whereas in this subsection we have exploited the similarities of the two derivations, in the next subsection we focus on the differences between them.

B. Comparison and generalization of the derivations

The analogy described above leads naturally to the question whether the contribution of each specific orbit is indeed quantitatively identical within the two approximation schemes. This comparison immediately runs into difficulty, because of the very different nature of the description of each scattering event, and the different types of scattering potential for which the two approximations are valid. In fact, a preliminary stage in the application of the diagrammatic method to a specific type of impurity is the modelling of the scattering by low-order perturbation with respect to an appropriate pseudopotential (which is usually different from the real potential). The analogous stage for the application of the semiclassical method would involve the construction of a *different* pseudopotential, such that, e.g., the physical size of each pseudoimpurity would be equal to the quantum scattering cross section of the real impurity.[43]

We thus find that the two different methods that led us in equivalent ways to the result discussed in this work [Eqs. (20) and (37)] were actually both based on the following three ingredients:

(i) A pseudopotential is chosen so as to reproduce the desired cross section, and hence the desired mean free path and diffusion constant.

(ii) Enough free motion between the scattering events is presumed ($k_F l \gg 1$), so that the orbits connecting these events are discrete and well separated.

(iii) Constructive interference between paths belonging to the same orbit, or to pairs of orbits related by symmetry, is allowed for.

We expect our result to hold for any situation in which the above conditions are met[44] (for instance, in a crystal, where the motion between scatterers is that of a Bloch electron).

The above claims of generality raise again the question of the domain of validity of the semiclassical result [Eq. (17)] and the application to diffusive systems [Eq. (20)]. As we have seen, for short times the semiclassical representation should be accurate (in fact, the pseudopotential is constructed so as to make it accurate), and therefore we expect the domain of validity to extend from $\hbar/E$ for the semiclassical Eqs. (17), (18), and from τ for the diffusive Eq. (20). For late times, the validity of the semiclassical derivation is unclear, but here the perturbative method provides an answer. It is found that evaluation of additional, higher-order, diagrams leads to corrections which become significant as the Heisenberg time t_H is approached. These additional diagrams correspond to the two-electron paths following orbits that are not identical, and deviate from one another at least over a short segment. Thus, we find that the failure of the leading-order diagrammatic result at times near t_H is due to the same type of "classical" approximation (omission of "off-diagonal" terms) as was introduced in the semiclassical approach. By analogy, we may therefore expect the semiclassical results to hold all the way up to times of order t_H, exactly as we expected on general grounds (due to the known leveling off of the form factor). This relies on the generality of the above three conditions, and does not necessarily imply the validity of the semiclassical expressions for the amplitude of a specific long orbit, Eq. (7).

V. APPLICATION TO PERIODICALLY DRIVEN SYSTEMS AND A NUMERICAL TEST

In this section we wish to present numerical evidence to support the results for a diffusive electron, Eq. (20). For this purpose, we must choose a discretized system. There are two natural systems to consider: Anderson's model[45] and the kicked rotor.[46] We prefer to use the kicked rotor because it avoids the problem of a finite bandwidth, and the resulting band edges, which make the appropriate averaging less well defined. Nevertheless, we modify the kicked rotor, making it more similar to the Anderson model as explained below (see also Ref. 47), so that the averaging is a random potential averaging as in the case of an electron (the extra τ dependence of the kicked rotor and the appearance of replica orbits are also avoided by this modification). The price paid is that the classical behavior of our system is now defined only in an ensemble-averaged sense (as in the Anderson model). Before presenting the specific system and the simulation results, we present an introduction including the basic definitions, for the sake of completeness.

A. The quasienergy spectral correlations

We consider the case of systems with periodically time-dependent Hamiltonians, and defer the discussion of the necessary use of a finite basis to the next subsection (both periodicity and finiteness were discussed by Dittrich and Smilansky[8]). As a prototype of such a system we can think of a free particle driven by a periodic external field. Such systems do not conserve energy, and so there is no need to distinguish between different energy hypersurfaces—for chaotic behavior the whole of phase space is filled. We can use the eigenvalues and eigenvectors of the evolution operator for one period, as a substitute for the spectrum and states in the energy preserving case. Within such a stroboscopic approach, the time variable is discretized as $t = n\tau$, where τ is the period of the system (it is analogous to the mean free time, which was denoted by τ in the earlier sections). The evolution operator becomes

$$G(x,y;n) = \sum_k \Psi_k^*(x) e^{-i\alpha_k n} \Psi_k(y) , \tag{38}$$

where Ψ_k are the eigenvectors of the one-step evolution operator, and α_k are the corresponding eigenphases (the eigenvalues are pure phases). These phases play the role of the eigenenergies in a time-independent system, but are defined only up to an arbitrary multiple of 2π. They are referred to as quasienergies. It is natural to define a "quasienergy spectral density" as

$$q(\alpha) = \sum_k \delta_p(\alpha - \alpha_k) , \tag{39}$$

where the δ_p function is defined to be 2π periodic. The Fourier transform is then discrete:

$$\tilde{q}(n)=\frac{1}{2\pi}\sum_k e^{-i\alpha_k n}$$
$$=\frac{1}{2\pi}\int dx\, G(x,x;n)\simeq\sum_j \tilde{A}_j(n)e^{i\tilde{S}_j(n)}, \quad (40)$$

where the last equation represents a semiclassical approximation as a sum over periodic orbits. Each periodic path is given by a starting point in phase space, and the list of $n-1$ points which corresponds to the motion of the system along $n-1$ field periods (assuming the system returns to the starting point after the nth period). A periodic orbit is given in the chaotic case by the ordered list of n points without specifying the starting point. In the integrable case the orbits form continuous curves or tori. Because of the additional freedom given by the lack of energy conservation, there is no restriction to $N>1$ for time-dependent chaotic systems.

The quasienergy spectral correlation function is then defined as

$$K(A,\alpha)=q\left[A+\frac{\alpha}{2}\right]q\left[A-\frac{\alpha}{2}\right], \quad (41)$$

and its Fourier transform is

$$\tilde{K}(A,n)=\frac{1}{2\pi}\int_0^{2\pi}d\alpha\, e^{-i\alpha n}K(A,\alpha)$$
$$=\sum_m \tilde{q}(n+m)\tilde{q}^*(n-m)e^{i2mA}. \quad (42)$$

This leads after averaging over $0<A\leq 2\pi$ to

$$\tilde{K}(n)=|\tilde{q}(n)|^2\simeq np(n) \quad (43)$$

(note that the first equality is an exact relationship; cf. Ref. 27). We have introduced the semiclassical approximation in the last equality, in analogy with Eq. (17), assuming that $p(n)$ is normalized appropriately. The factor of n again arises from interference within each orbit, but here the orbits are indeed a set of n discrete paths, so there is no problem with the continuous t parameter (this interference has been noted already in Ref. 8).

Again, for a time symmetric evolution the interference of time-reversed paths introduces a further factor of 2 (except for special cases such as $n=2$, when the path coincides with its time reverse).

As a result of our definition of the averaging of $\tilde{K}(A,n)$ over all A's and without averaging over n's, $\tilde{K}(n)$ is equal to the absolute square of a well-defined $\tilde{q}(n)$. The ensemble distribution of this quantity, $\tilde{q}(n)$, will generally be a Gaussian centered at the origin of the complex plane (compare with Ref. 28). This implies large fluctuations in $\tilde{K}(n)$, with the standard deviation equal to the mean (such fluctuations are indeed obtained in the simulations to be presented below).

B. The modified kicked rotor

One specific example of a periodically time-dependent Hamiltonian is that of the kicked rotor,[46] which reads

$$H(l,\theta)=\frac{l^2}{2}+k\sin(\theta)\sum_n \delta(t-n\tau) \quad (44)$$

(we use sin instead of the more customary cos in order to avoid some unnecessary phases in the matrix elements). Physically, it corresponds to a rotator of unit moment of inertia, where θ is its angular position, l is its angular momentum, k is the kicking strength, and τ is the time interval between successive kicks (l and k are measured in units of $\hbar$, and τ is measured in units of the natural basic frequency of the quantized rotor, which is $\sim 1/\hbar$). Classically, the evolution during each period yields a mapping from $(\theta_n,\tau l_n)$ to $(\theta_{n+1},\tau l_{n+1})$, which depends on the single parameter $K_{cl}=\tau k$ (the factor τ appears so that time is measured here with respect to the kicking period). The system behaves as a perturbed rotator for $K_{cl}\ll 1$, and exhibits chaotic diffusion in l space for $K_{cl}\gg 1$ (because successive values of θ become uncorrelated). For generic values of τ, this diffusion is suppressed quantum mechanically, and Anderson-like localization in l space is observed,[46] with a localization length $\xi\propto k^2$ (in the present paper we will consider only cases in which the localization is not relevant because the size of the system is smaller, $L\lesssim\xi$).

The quantum evolution operator for one period is

$$\hat{U}=\exp(-ik\sin(\hat{\theta}))\exp\left[-\frac{i}{2}\tau\hat{l}^2\right], \quad (45)$$

which in the l (angular momentum) representation reads

$$U_{l,l'}=J_{l-l'}(k)\exp\left[-\frac{i}{2}\tau l^2\right] \quad (46)$$

($J_{l-l'}(k)=\int\exp[ik\sin(\theta)-i(l-l')\theta]d\theta/2\pi$ is the Bessel function). This evolution is easy to simulate numerically because the operator has factors which are diagonal in either l or θ space, and the transformation between these two representations of the state vector can be quickly effected by use of fast-Fourier-transform (FFT) algorithms (in the discrete case).

For the purpose of numerical simulation, we must choose a finite discrete basis, and in order to observe diffusion we must work in angular momentum space. Using the Fourier-transform technique implies periodic boundary conditions for this "sample of l space" (in fact, the matrix elements are now given by a discrete sum approximation of the Bessel function integrals). The picture becomes analogous to a "time-dependent tight-binding model," in which each site corresponds to a value of l, and the system is periodically perturbed by a "kick" that may shift a particle to a nearby site (mixes the values of the wave function on nearby sites). The quasienergy values of the individual sites $\phi_l=\tau l^2/2_{\mathrm{mod}2\pi}$, $l=1,\ldots,L$, may be considered as pseudorandom,[47] and in this work we take them as completely random $\phi_l\in[0,2\pi]$. As mentioned above, we have thus modified the kicked rotor system, and made it more similar to the Anderson model.

The use of a random distribution of ϕ_l enables the definition of an "ensemble-averaged classical behavior" for this "kicked tight-binding model." Introducing random, uncorrelated site quasienergies implies a complete "dephasing" in the l basis at each time step (obviously

this "dephasing" is due to the averaging, and no inelastic scattering is implied). In a sense, this is the opposite of the semiclassical limit, where small $\hbar$ would lead to a smooth dependence of ϕ_l on l. It enables the definition of "quantum paths" and corresponding probabilities, in complete analogy with the semiclassical analysis: we define j, a "quantum periodic path" of length n to consist of an ordered list of n discrete sites in the l basis, $j=\{l_1,l_2,\ldots,l_n\}$. The corresponding amplitude is $A_j=\prod_{i=1}^{n}J_{l_i-l_{i-1}}(k)$, and the "action" is $S_j=\sum_i\phi_{l_i}$, with l_0 and l_n identified. We find that the representation of the quantum probability amplitude to perform periodic motion as a sum over paths, $\tilde{q}(n)=\sum_j A_j\exp(iS_j)$, is *exact*. We are led to define the "classical evolution" of an initial distribution δ_{l-l_0} into an eventual distribution δ_{l-l_n} after n steps, in a way such that the path j is followed with a probability $p_j=\prod_i|J_{l_i-l_{i-1}}(k)|^2$ (at least in an ensemble-averaged sense). The connection $\tilde{K}(n)=np(n)$ will now follow by noting that the n paths that are related to each other by a cyclic permutation of the $\{l_i\}$ have identical amplitudes and phases, and naturally form an "orbit" (the factor of 2 for the time-reversal symmetric cases will also follow).

Note that here the only questionable step is the omission of off-diagonal terms in the orbit sum. This step may be justified by claiming that the correlations should be small if the site quasienergies are uncorrelated, and the kicking parameter k is large (this corresponds to the requirement of a large mean free path $k_Fl\gg1$). Nevertheless, since the form factor cannot increase without limit, it is clear that subtle correlations[23] in the off-diagonal terms will amount to an important contribution to $\tilde{K}(n)$, for times $n>n^*$ with n^* denoting the appropriate "Heisenberg time" (or a shorter time in the case of localization).

We have thus defined the "classical evolution" as a random walk on the lattice of l sites, with the probability of jumping Δl sites at each step given by $|J_{\Delta l}(k)|^2$. One may check that this evolution is "unitary," $\sum_{\Delta l}|J_{\Delta l}(k)|^2=1$, and that after a short time it results in diffusion, with a constant of $D=(1/2\tau)\sum_{\Delta l}\Delta l^2|J_{\Delta l}(k)|^2=k^2/4\tau$. For large values of K_{cl} this is identical with the classical diffusion constant (for smaller values of K_{cl} deviations due to some residual correlations in the generally chaotic behavior exist[48]). The fact that the analysis of this problem leads to the same result, $\tilde{K}(n)=np(n)\sim\sqrt{n}$ for both the semiclassical and the quantum cases, is a striking example of the generality alluded to in the preceding section.

The results for $\tilde{K}(n)$ in our one-dimensional discrete system are shown in Fig. 4. It is seen that the averaged $\tilde{K}(n)$ follows the theoretical result of Eq. (43). We note that the factor $p(n)$ was calculated from a classical simulation based on the exact form of the quantum kick, $|J_{\Delta l}(k)|^2$ (and not from a diffusion equation approximation), the symmetry factor 2 was corrected for the first few steps to exclude self-symmetric paths, and the n factor was replaced by the full GOE form factor so that the saturation of the results at large n would be accounted for

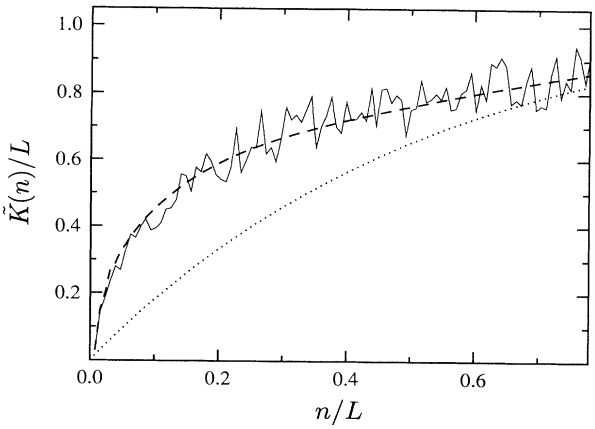

FIG. 4. Results of simulation of a one-dimensional, time periodic, diffusive system: The averaged $\tilde{K}(n)$ (continuous line) from 230 realizations of a 128-site modified kicked rotor, with a kicking strength of $k=8$. The results clearly follow the present theory (dashed line), which is also compared here with the GUE random matrix result or the $p(n)=$const case (dotted line). Both axes are scaled by the number of sites in the system.

(at least in their general form). All of these modifications would be irrelevant for a larger system, which would show just $t^{1/2}$ behavior [Eq. (20)] for times up to the ergodic time, and linear ($\propto t$) behavior between the ergodic time and the Heisenberg time n^* (in the case presented in Fig. 4 the last range is vanishingly short, but it will appear in the next example). We have chosen the parameters $k=8$ (the kicking strength) and $L=128$ (the number of sites in the mesh) so as to conform with the requirements $k\gg1$ (this is analogous to $k_Fl\gg1$) and $k\ll L\sim\xi$ (diffusive, nonlocalized behavior). By repeating the calculations with different values of L and k, we have checked that the localization, which is marginal here since $L\sim\xi$, has no influence on the results plotted [although it does influence other properties which are more sensitive than $\tilde{K}(n)$].

We have also performed simulations for a two-dimensional system, for which $\tilde{K}\sim$const for early times. This system is obtained by simply taking the above modified kicked rotor, and doubling the number of degrees of freedom. It consists of a two-dimensional (l_1,l_2) array of random quasienergy sites, kicked by the operator

$$\exp\{-ik[\sin(\hat{\theta}_1)+\sin(\hat{\theta}_2)]\}\ , \tag{47}$$

which is diagonal in the (two-dimensional) Fourier-transform representation (θ_1,θ_2). Note that here the fact that we chose random site quasienergies becomes important, because if we were to use the separable form depending on l_1 and l_2 separately, the problem would separate into two one-dimensional kicked rotors (of course there are other ways to overcome this[49]). It is hard to visualize the corresponding classical system, although the Hamiltonian can easily be written. The modified finite discrete quantum system is best considered simply as a tight-binding two-dimensional array, with a periodically time-dependent Hamiltonian. The analysis

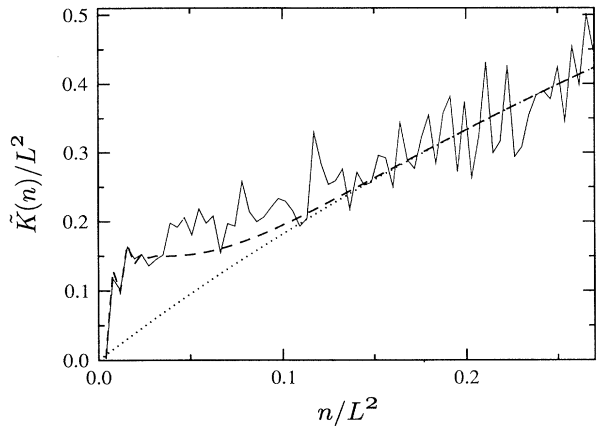

FIG. 5. Simulation results for a two-dimensional 16×16 system, averaged over 60 realizations, with kicking parameter $k=2$. Notation as in Fig. 4.

of the "quantum paths" may be carried out in this case too.

The numerical results, for a kicking strength $k=2$ and system size of $L\times L=16\times16$ sites, are presented in Fig. 5. Here too we have attempted, within the limitations of computation resources, to choose parameters such that $1\ll k\ll L\lesssim\xi$ [here ξ is exponential in k (Ref. 49)]. The agreement between theory and simulation in the two-dimensional case is also good, and presumably could be improved by having better statistics and larger values of the kicking parameter k, i.e., larger systems.

VI. CONCLUSION AND FUTURE RESEARCH

We have discussed the connection between the spectral form factor, which determines several important physical quantities in mesoscopic samples, and the classical probability to perform periodic motion. Our main result is that the spectral form factor is proportional to t times the classical probability to perform periodic motion, with the factor of t resulting from adding the quantum amplitudes, rather than the classical probabilities, of the "t periodic paths" that constitute an orbit. This result has an extremely wide range of applicability: it can be used for any specific geometry and potential, provided only that the classical motion is chaotic. This contrasts with the diagrammatic approach, in which the averaging over the positions of the impurities is an essential element from the outset (in both approaches there is also a limitation on the type of potential for which an individual scattering event is approximated well, but this limitation can be relaxed in both cases by the use of different pseudopotentials). We point out that the classical probability to return to the starting point, which plays a crucial role in the well-known weak-localization correction to the conductivity,[11,41,42] is similar to the classical probability for periodic motion used here. Although in principle the former is contributed to by any path that returns to its initial position, while the latter requires that the path return also to its initial momentum, the difference between the two often becomes a simple constant factor upon averaging over the sample or the ensemble.

Another important ingredient is the diffusive behavior of the probability to perform periodic motion. We claim that both the interference and the diffusion are very general phenomena, and therefore our results should hold independent of the details of the scattering potential, and in some cases even the size of $\hbar$ (as long as the disorder is weak, $k_F l\gg1$, and there are no Anderson-localization effects). The availability of different derivations of the same result not only supports its generality, but also provides additional physical insight. For example, we have given a physically motivated argument for the choice of the dominant perturbation-theory diagrams in the calculation of the spectral correlation function.

One interesting avenue for future research would be a more thorough examination of the domains of validity, and accuracy of this picture. At present, the only limitation on the domain of validity appears to be $t\lesssim t_H$ (for a correct treatment of times $t\gtrsim t_H$ other approaches are necessary, e.g., the field theory of Ref. 3). Both the semiclassical and the diagrammatic approaches provide techniques to calculate corrections to the standard results (integration near caustics, high-order diagrams), which appear to be of a different nature. But the generality of the results leads to the suspicion that there may exist entities analogous to "classical paths" and their "quantum amplitudes" and "classical contributions," such that the "semiclassical" connections that we have found would be exact. Thus far we have only been able to define such "quantum paths" in the discrete, time-periodic case (Sec. V B).

The same situation also calls for another approach: Imagine that the density of states $d(\epsilon)$ is written exactly as a sum over discrete contributions of the semiclassical type; this immediately implies, as we have seen, that these contributions will be correlated for late times.[23] An example of such an exact sum is the sum of contributions to the path integral from different winding numbers, in the case of the mesoscopic rings discussed above. At present, the intricate correlations between the terms can only be appreciated by noting that the evolution is unitary and limited to a compact energy surface. It is desirable to develop models in which these correlations can be studied explicitly. This may also lead to a better "semiclassical" understanding of Anderson localization, since it is possible that the same effects that cause the deviation from the simple "classical" sum discussed in this work will also cause the deviations implied by localization. One possibility to attack this problem is through a careful comparison with renormalization-technique approaches.[50]

Finally, we return to the topic of applications to mesoscopic systems. The formula for the spectral form factor may be applied easily in many cases (we have discussed three applications), since all that is needed is a knowledge of the system's classical behavior. The results for diffusing electrons are quite general, and form a new type of universality class (not as general as the random matrix ensembles). Still, details of specific cases remain to be worked out, such as the influence of specific geometries and applied fields. The crossover regions between two regimes described by different random matrix

ensembles also warrants further study (generalizations of our Sec. III B). We have considered the application to the single-particle spectral correlations of mesoscopic systems, in which each electron moves in the self-consistent field of the others, but our main result, Eq. (18), should hold generally. An evaluation of the classical probability to perform periodic motion, $p(t)$, for the many-body problem should lead to the spectral correlations of the full many-particle Hamiltonian.

ACKNOWLEDGMENTS

The authors wish to thank A. Altland, B. L. Altshuler, H. Baranger, M. V. Berry, E. B. Bogomolny, E. Brezin, B. Derrida, T. Dittrich, E. Doron, Y. Gefen, S. Levit, J. M. Robbins, and A. Stern for helpful discussions. This project was supported by the Minerva Foundation (Munich, Germany) and the German Israel Foundation (GIF) Jerusalem.

APPENDIX: PERFORMING THE PHASE SPACE INTEGRALS

In this appendix, we rederive the expression for the classical probability associated with a periodic orbit j [Eq. (15)], and compare it with that for the quantum amplitude corresponding to the same orbit [Eq. (7)].

In order to evaluate the contribution of a periodic orbit j to the classical probability to perform periodic motion [Eq. (14)], it will turn out to be convenient to use a coordinate system which is tailored to the specific orbit j. The $2N$ new phase-space coordinates include two coordinates which span the periodic orbit sheet itself: the energy (or Hamiltonian) H, and the conjugate "time" variable T, which measures the distance along the orbit in units of the time required to traverse it. At each point of (H,T) one may consider the transverse hyperplane, which is called a Poincaré section. It is spanned by $N-1$ canonical coordinates Q and momenta P, taking the periodic orbit as the origin.[17] This set of canonical coordinates is chosen so that the Hamiltonian function is independent of all of them except for H, and thus they are all constants of the classical motion, except for T. The price paid is that it is multivalued, in the sense that with the evolution around and around a path near the periodic orbit, the same transverse coordinates (P,Q) refer to different points in phase space after each revolution. The Poincaré map $F(P,Q)$ is defined as the transformation from a point on a certain Poincaré section to its image generated by the Hamiltonian flow after one revolution. This means that the phase-space point $(H,T+T_j,P,Q)$ coincides with the point $(H,T,F(P,Q))$, albeit on a different branch of the coordinate system (as above, T_j is the orbit's period, and may depend on H). The monodromy matrix M_j is that associated with the linearized form of the Poincaré map near the periodic orbit itself. Note that, as the transverse coordinates (P,Q) are constants of the motion, the Poincaré map F is independent of the position along the orbit T.

Rewriting the integral of Eq. (14) in the new coordinate system, we have

$$P_j(E,t)=\int_{\Gamma_j} dQ_0 dP_0 dT_0 dH_0 \times\delta(H_0-E)\delta^{N-1}(Q_0-Q_t) \times\delta^{N-1}(P_0-P_t)\delta(T_0-T_t)\ . \tag{A1}$$

The integration over the energy coordinate H_0 is trivial. For the time evolution we can simply write $T_t=T_0+t$, with the other coordinates remaining time independent. We must now transform back to the original branch of our coordinate system by using the Poincaré map:

$$P_j(E,t)=\int_{\Gamma_j} dQ_0 dP_0 dT_0 \delta^{2N-2}[(Q_0,P_0)-F(Q_0,P_0)]\delta(T_0+t-T_j-T_0)\ . \tag{A2}$$

The δ function over times becomes independent of the integration variables, and can be taken out of the integral. The integration over T_0 becomes a trivial integration over a constant integrand, and gives just the size of the integration region, $T_{j'}$ (again, j' is the primitive orbit corresponding to j). The integration over the remaining $(2N-2)$-dimensional δ function gives just the inverse of the determinant of the derivatives of the argument, and so we finally find

$$P_j(E,t)=\delta(t-T_j)T_{j'}|\det(M_j-I)|^{-1}\ . \tag{A3}$$

This is exactly Eq. (15)

We now wish to compare this derivation with that of the quantum amplitude, Eq. (7). The standard method[17,18] for deriving the amplitudes and phases of Gutzwiller's sum involves the straightforward application of the stationary phase approximation to the integrations involved in Eq. (3). It is also possible to rewrite the trace of the propagator as a phase-space integral, using either the Wigner representation[51] or a coherent-state representation.[52] We will not go into the details of these derivations here, but we point out that they all share a common feature with the classical derivation given above: the contributions to the integral correspond to periodic orbits, and the integration over the length of the orbit is singled out as an integration over a constant integrand which simply gives the length of the integration region $T_{j'}$. The explicit appearance of the monodromy matrix is not as transparent, but can be understood intuitively in analogy with the usual semiclassical results for the propagator: the semiclassical amplitude is equal (apart from the Maslov index) to the square root of the classical probability density.

Finally we emphasize that the "constructive interference" of the contributions of different points on the same periodic orbit differs from the usual notion of constructive interference between a discrete set of amplitudes. Here the contributions of different points are integrated

over, and it is necessary to go through the detailed derivations discussed here to see how the integrations are separated into transverse and longitudinal (timelike) coordinates. The comparison of these derivations provides the proof that the continuous infinity of classical paths belonging to the orbit j can indeed be considered as "T_j different paths," with identical actions S_j and amplitudes $|\det(M_j-I)|^{-1/2}/2\pi\hbar$.

---

*Previously known as Nathan Freed.

[1]B. L. Altshuler and B. I. Shklovskii, Zh. Eksp. Teor. Fiz. **91**, 220 (1986) [Sov. Phys. JETP **64**, 127 (1986)].

[2]F. J. Dyson, J. Math. Phys. **3**, 140 (1962); **3**, 1191 (1962); F. J. Dyson and M. L. Mehta, *ibid.* **4**, 701 (1964); M. L. Mehta, *Random Matrices* (Academic, New York, 1967).

[3]See, e.g., K. B. Efetov, Adv. Phys. **32**, 53 (1983).

[4]D. J. Thouless, Phys. Rev. Lett. **39**, 1167 (1977).

[5]M. C. Gutzwiller, J. Math. Phys. **12**, 343 (1971).

[6]M. V. Berry, Proc. R. Soc. London Ser. A **400**, 229 (1985).

[7]J. H. Hannay and A. M. Ozorio de Almeida, J. Phys. A **17**, 3429 (1984).

[8]T. Dittrich and U. Smilansky, Nonlinearity **4**, 59 (1990); **4**, 85 (1990).

[9]U. Smilansky, S. Tomsovic, and O. Bohigas, J. Phys. A **25**, 3261 (1992).

[10]E. Doron, U. Smilansky, and T. Dittrich, Physica B **179**, 1 (1992).

[11]S. Chakravarty and A. Schmid, Phys. Rep. **140**, 193 (1986).

[12]See, e.g., P. A. Lee, A. D. Stone, and H. Fukuyama, Phys. Rev. B **35**, 1039 (1987).

[13]M. Buttiker, Y. Imry, and R. Landauer, Phys. Lett. **96A**, 365 (1983); R. Landauer and M. Buttiker, Phys. Rev. Lett. **54**, 2049 (1985).

[14]An earlier attempt to apply semiclassical considerations to this problem is Y. Imry, in *Quantum Coherence in Mesoscopic Systems,* Vol. 254 of *NATO Advanced Study Institute Series B: Physics,* edited by B. Kramer (Plenum, New York, 1991), p. 221.

[15]H. Cheung, E. K. Riedel, and Y. Gefen, Phys. Rev. Lett. **62**, 587 (1989). Note that the numerical coefficient in our Eq. (23) is larger by a factor of 3 than the result of this reference (the assumption of three dimensions is implicit there), due to the omission of "two-ladder" diagrams; see F. von Oppen and E. K. Riedel, *ibid.* **66**, 86 (1991). An analogous result has been derived in the related context of the SNS junction in B. L. Altshuler and B. Z. Spivak, Zh. Eksp. Teor. Fiz. **92**, 609 (1987) [Sov. Phys. JETP **65**, 343 (1987)].

[16]A. Schmid, Phys. Rev. Lett. **66**, 80 (1991); **66**, 1379(E) (1991); B. L. Altshuler, Y. Gefen, and Y. Imry, *ibid.* **66**, 88 (1991). Note the error in the sign of Eq. (6) in the last reference; the physical discussion following it is based on the correct sign, however.

[17]A. M. Ozorio de Almeida, *Hamiltonian Systems: Chaos and Quantization* (Cambridge, New York, 1988).

[18]M. C. Gutzwiller, *Chaos in Classical and Quantum Mechanics* (Springer-Verlag, Berlin, 1990).

[19]O. Bohigas, M. J. Giannonni, and C. Schmit, Phys. Rev. Lett. **52**, 1 (1984).

[20]A. J. Lichtenberg and M. A. Lieberman, *Regular and Stochastic Motion* (Springer-Verlag, New York, 1983).

[21]J. M. Robbins, Nonlinearity **4**, 343 (1991).

[22]P. V. O'Connor, S. Tomsovic, and E. J. Heller, Physica D **55**, 340 (1992).

[23]N. Argaman, E. Doron, J. Keating, A. Kitaev, M. Sieber, and U. Smilansky (unpublished).

[24]See, e.g., M. V. Berry and J. P. Keating, J. Phys. A **23**, 4839 (1990); J. P. Keating, Proc. R. Soc. London Ser. A **436**, 99 (1992); E. B. Bogomolny, Comments At. Mol. Phys. **25**, 67 (1990); P. Cvitanovic and B. Eckhardt, Phys. Rev. Lett. **63**, 823 (1989); E. Doron and U. Smilansky, Nonlinearity (to be published); R. Aurich and F. Steiner, Proc. R. Soc. London (to be published).

[25]See, e.g., N. L. Balasz and A. Voros, Phys. Rep. **143**, 109 (1986).

[26]See, e.g., M. A. Sepulveda, S. Tomsovic, and E. J. Heller, Phys. Rev. Lett. **69**, 402 (1992). In this reference it is suggested that $t_{SC}\sim\hbar^{-1/3}$ for the accuracy of the propagator, while in Ref. 23 it is shown that, at least in some cases, $t_{SC}>t_H$ for the accuracy of the spectral form factor.

[27]If $\tilde{K}(E,t)$ is written in terms of $\tilde{d}(t)$, and then averaged over a Gaussian distribution over the small ranges ΔE and Δt, the following exact relationship for the averaged $\tilde{K}$ results:

$$\tilde{K}(E,t)=\int dt_1\tilde{d}(t_1)\exp(iEt_1/\hbar)\times\int dt_2\tilde{d}^*(t_2)\exp(-iEt_2/\hbar)F(t_1,t_2;t)\,,$$

with

$$F(t_1,t_2;t)=\exp[-(t_1-t_2)^2\Delta E^2/2\hbar^2]\times\frac{1}{\sqrt{2\pi}\Delta t}\exp\{-[t-\tfrac{1}{2}(t_1+t_2)]^2/2\Delta t^2\}$$

(note that Δt and ΔE do not necessarily obey an uncertainty relationship because they refer to two different variables of $\tilde{K}$). If the semiclassical approximation is now inserted and F may be considered as slowly varying [i.e., $\hbar/t\ll\Delta E\ll E'$, and $\hbar/E'\ll\Delta t\ll t$, where E' signifies the sensitivity of the action to changes in the time, $E'=\sqrt{\hbar\partial E_j/\partial t}=\sqrt{\hbar/(d^2S_j/d\epsilon^2)}$], we recover Eq. (10) with $F(T_j,T_k;t)$ instead of the δ function. If either of T_j or T_k is not within $\Delta t+\hbar/\Delta E$ from t (we have assumed Δt, $\hbar/\Delta E\ll t$), the F factor decays in a Gaussian fashion, rendering the effective number of terms in Eq. (10) finite, and thus solving the convergence problem. We will use an analog of this derivation in Sec. V.

[28]It is worthwhile to note the expected magnitude of the fluctuation of $\tilde{K}(E,t)$ of a specific system from the ensemble-averaged value. The standard deviation $(\langle\tilde{K}^2\rangle-\langle\tilde{K}\rangle^2)^{1/2}$ may be estimated for $t\ll t_H$, by assuming the absence of correlations between the actions in the semiclassical expression for $\tilde{K}$. It depends on the amount of self-averaging included in $\tilde{K}$, which is specified by the product $\Delta E\Delta t$, and turns out to be small if $\Delta E\Delta t\gg\hbar$. A simple demonstration can be given by use of the definitions in Ref. 27, when $\Delta E\Delta t=\hbar/2$. In this case the factor $F(t_1,t_2;t)$ factorizes and $\tilde{K}(E,t)$ may be written as a product of an integral and its complex conjugate. This integral may be written semiclassically as a sum of terms which are assumed to be uncorrelated, and therefore its value is distributed according to a Gaussian distribution around the origin in the complex plane. This means that $\tilde{K}(E,t)$, which is proportional to the absolute

value squared of the integral, will have a Poissonian distribution, with standard deviation equal to the mean. A similar type of argument also works for late times $t \gg t_H$, where the correlations between the energy eigenvalues may be neglected.

[29]See, e.g., M. V. Berry, in *Chaos and Quantum Physics*, Proceedings of the Les Houches Summer School in Theoretical Physics, Session LII, 1989, edited by M. J. Giannoni, A. Voros, and J. Zinn-Justin (North-Holland, Amsterdam, 1991), p. 251.

[30]L. P. Levy, G. Dolan, J. Dunsmuir, and H. Bouchiat, Phys. Rev. Lett. **64**, 2074 (1990).

[31]V. Chandrasekhar, R. A. Webb, M. J. Brady, M. B. Ketchen, W. J. Gallagher, and A. Kleinsasser, Phys. Rev. Lett. **67**, 3578 (1991).

[32]S. Oh, A. Yu. Zyuzin, and R. A. Serota, Phys. Rev. B **44**, 8858 (1991); B. L. Altshuler, Y. Gefen, Y. Imry, and G. Montambaux (unpublished).

[33]In order to obtain the exponentially small term within the semiclassical approach, one must keep track of the contributions of the few stable orbits which may still exist in a disordered sample.

[34]A. Altland, S. Iida, A. Müller-Groeling, and H. A. Weidenmüller, Europhys. Lett. (to be published); Ann. Phys. (to be published).

[35]N. Dupuis and G. Montambaux, Phys. Rev. B **43**, 14 390 (1991); see also O. Bohigas, in *Chaos and Quantum Physics* (Ref. 29), p. 87, Sec. 6, and references therein.

[36]B. L. Altshuler and A. G. Aronov, Pis'ma Zh. Eksp. Teor. Fiz. **33**, 515 (1981) [JETP Lett. **33**, 499 (1981)]. A detailed explanation of the relationship between the gauge and the boundary conditions may be found in Ref. 32.

[37]Note that although the averaging over the symmetry-breaking phases is identical here and in the case of weak localization, there are also some differences, e.g., the necessity for a special treatment of the end points of the paths (Appendix D of Ref. 11) as opposed to our case of periodic orbits without ends. Another important difference is in the way the spins are summed over.

[38]Y. Gefen, A. Aharony, and S. Alexander, Phys. Rev. Lett. **50**, 77 (1983).

[39]B. Derrida and Y. Pomeau, Phys. Rev. Lett. **48**, 627 (1982); Ya. G. Sinai, *Proceedings of the Sixth International Conference on Mathematical Physics, Berlin, 1981* (Springer-Verlag, Berlin, 1982), p. 12.

[40]The standard reference is A. A. Abrikosov, L. P. Gorkov, and I. E. Dzyaloshinski, *Methods of Quantum Field Theory in Statistical Physics* (Prentice-Hall, New Jersey, 1963); A modern textbook is J. W. Negele and H. Orland, *Quantum Many-Body Systems* (Addison-Wesley, New York, 1988).

[41]A. I. Larkin and D. E. Khmelnitskii, Usp. Fiz. Nauk **136**, 536 (1982) [Sov. Phys. Usp. **25**, 185 (1982)]; D. E. Khmelnitskii, Physica B **126**, 235 (1984).

[42]G. Bergmann, Phys. Rep. **107**, 1 (1984).

[43]Even after different pseudopotentials are chosen for the two approximations, the semiclassical and the perturbative formulas for the amplitude of a specific orbit in a specific member of the impurity averaging ensemble should not be expected to coincide. This is due to the different ways in which shadowing (which is necessary to preserve unitarity) is treated: in the semiclassical approach, an orbit connecting a specific set of scatterers may (or may not) be completely screened by an intervening impurity; in the perturbative approach there is a gradual reduction of the amplitude due to forward scattering on intervening impurities (which in that scheme is the only process that involves second-order perturbation scattering, and gives exactly the correct reduction due to the optical theorem). Note that in the "semiclassical" approach of Ref. 11 the reduction is also gradual, as in the perturbative approach.

[44]In fact, there exists numerical evidence supporting the generality of the semiclassically derived result, Eq. (20), even when it is applied to the region in which $\hbar$ is not small. One example is the kicked rotor mentioned in the next section (another is Ref. 10). The results (for the case with $\phi_l = \tau l^2/2$) do not depend sensitively on $\hbar$, and simulations with relatively large values of $\hbar$ are sometimes used to demonstrate semiclassically derived relationships. This can also be done for our case, and results very similar to Figs. 4 and 5 are obtained (simulations with small values of $\hbar$ were not attempted because they require a very large computation effort).

[45]For a modern exposé see, e.g., H. Kamimura and A. Aoki, *The Physics of Interacting Electrons in Disordered Systems* (Clarendon, Oxford, 1989), pp. 97–102.

[46]B. Chirikov, Phys. Rep. **154**, 77 (1979); see also F. M. Izrailev, *ibid.* **196**, 299 (1990), and Ref. 8.

[47]M. Griniasty and S. Fishman, Phys. Rev. Lett. **60**, 1334 (1988).

[48]See, e.g., D. L. Shepelyanski, Phys. Rev. Lett. **56**, 677 (1986).

[49]E. Doron and S. Fishman, Phys. Rev. A **37**, 2144 (1988); Phys. Rev. Lett. **60**, 867 (1988).

[50]See, e.g., P. Wolfle and D. Vollhardt, Phys. Rev. Lett. **48**, 699 (1982).

[51]M. V. Berry, Proc. R. Soc. London Ser. A **423**, 219 (1989).

[52]See, e.g., R. G. Littlejohn, Phys. Rep. **138**, 193 (1986); J. Math. Phys. **31**, 2952 (1990).